

Neurite Orientation Dispersion and Density Imaging of The Nigrostriatal Pathway in Parkinson's Disease: Retrograde Degeneration Observed by Tract-profile Analysis

メタデータ	言語: English 出版者: 公開日: 2020-03-20 キーワード: 作成者: Andica, Christina メールアドレス: 所属:
URL	https://jair.repo.nii.ac.jp/records/2002486

Title:

Neurite Orientation Dispersion and Density Imaging of the Nigrostriatal Pathway in

Parkinson's Disease: Retrograde Degeneration Observed by Tract-Profile Analysis

Authors:

Christina Andica^{1, *}, Koji Kamagata¹, Taku Hatano², Ayami Okuzumi², Asami Saito¹, Misaki

Nakazawa¹, Ryo Ueda^{1, 3}, Yumiko Motoi², Kouhei Kamiya⁴, Michimasa Suzuki¹, Masaaki

Hori¹, Kanako K Kumamaru¹, Nobutaka Hattori², and Shigeki Aoki¹

Affiliations:

¹Department of Radiology, Juntendo University Graduate School of Medicine

2-1-1 Hongo, Bunkyo-ku, Tokyo, 113-8421, Japan

²Department of Neurology, Juntendo University Graduate School of Medicine

2-1-1 Hongo, Bunkyo-ku, Tokyo 113-8421, Japan

³Department of Radiological Sciences, Graduate School of Human Health Sciences, Tokyo

Metropolitan University

7-2-10 Higashiogu, Arakawa-ku, Tokyo 116-8551, Japan

⁴Department of Radiology, Graduate School of Medicine, The University of Tokyo

7-3-1 Hongo, Bunkyo-ku, Tokyo, 113-0033, Japan

*Corresponding author:

Department of Radiology, Juntendo University Graduate School of Medicine, 2-1-1 Hongo,

Bunkyo-ku, Tokyo, 113-8421, Japan. E-mail address: andicach@gmail.com

Keywords:

Diffusion Tensor Imaging; Neurite Orientation Dispersion and Density Imaging; Parkinson's disease; Nigrostriatal Pathway; Retrograde Degeneration; Tract-profile Analysis.

Abstract

Introduction: Parkinson's disease (PD) is marked by the degeneration of dopaminergic neurons in the nigrostriatal pathway (NSP). We aimed to identify the microstructural changes in the NSP of PD patients using neurite orientation dispersion and density imaging (NODDI).

Methods: NSPs of 29 PD patients, who were retrospectively selected from patients previously admitted to our institution, and 29 age- and gender-matched healthy controls were isolated via deterministic tractography. The NODDI indices, intracellular volume fraction (Vic), orientation dispersion index (OD), and isotropic volume fraction (Viso) were compared between the two groups. The significant results were assessed with a tract-profile analysis.

The correlation between indices and disease duration or motor symptom severity was evaluated with the Pearson's correlation test.

Results: The contralateral distal Vic ($p = 0.00028$) of the nigrostriatal pathway was significantly lower in PD patients than in healthy controls. No correlations were detected between any of the indices and disease duration or motor symptom severity.

Conclusions: NODDI can be used to identify retrograde degeneration of the NSP in PD patients and might be useful for monitoring the disease progression of PD.

1. Introduction

Parkinson's disease (PD) is a neurodegenerative movement disorder characterized by the degeneration of dopaminergic neurons projecting from the substantia nigra pars compacta (SNpc) to the corpus striatum, which is known as the nigrostriatal pathway (NSP) [1, 2]. The loss of nigrostriatal projections is presumed to be the cause of the motor symptoms observed in PD [1]. Altered protein handling plays a key role in the etiopathogenesis of PD. The aggregation of presynaptic protein α -Synuclein was shown to be the major component in the accumulation of Lewy bodies and neurites, which are pathological hallmarks of neuronal degeneration in PD [3-5]. Lewy neurites are found more abundantly and earlier in the distal axons and may impair retrograde axonal transport, leading to neuronal loss [5, 6]. Based on these findings, it was assumed that the progression of PD involves a dying back process that begins in the distal axons [2, 4].

Diffusion tensor imaging (DTI) has been used to examine nigrostriatal degeneration; however, previous studies [7, 8] have failed to demonstrate sufficient clinical diagnostic accuracy and reliability, likely due to the limitations of DTI, which include 1) the diffusion of water molecules in living tissue exhibits a non-Gaussian distribution; and 2) despite its sensitivity, fractional anisotropy (FA) cannot be used to determine the specific pathological changes of the NSP in PD [7, 8]. Decreased FA can be caused by a reduction in neurite density, an increase in the dispersion of neurite orientation distribution, as well as

demyelination [7, 8].

In this study, neurite orientation dispersion and density imaging (NODDI) was applied to examine the NSP. NODDI enables the quantification of neurite density and orientation dispersion with an orientation-dispersed cylinder model and Watson distribution [8, 9]. NODDI indices, the intracellular volume fraction (V_{ic}) and the orientation dispersion index (OD), are assumed to describe more specific microstructural changes and represent changes in FA [7-9].

We hypothesized that NODDI could be used to identify the retrograde degeneration of the NSP in PD as a useful marker of disease progression. To test this hypothesis, the usefulness of NODDI analysis to examine the NSP was compared between PD patients and healthy controls.

2. Materials and methods

2.1 Subjects

This study was a retrospective case-control study included 58 subjects (29 PD patients and 29 healthy controls). The characteristics of all study participants are listed in Table 1. PD patients were previously admitted to our institution and diagnosed by movement disorders specialists based on the UK Parkinson's Disease Society Brain Bank criteria [10] and had stage I, II, or III PD according to the Hoehn and Yahr scale [11]. All PD patients

remained free from atypical parkinsonism and exhibited a good response to anti-parkinsonian therapy for ≥ 18 months after diagnosis. All patients were taking levodopa in combination with a dopamine decarboxylase inhibitor (benserazide or carbidopa) at the time of magnetic resonance imaging (MRI) and clinical examination. Age- and gender-matched healthy subjects with no history of neurologic or psychiatric disorders and having no abnormal signals on structural MRI were recruited as a control group. Although some of the healthy volunteers had normal age-related brain atrophy, none had pathological atrophy indicative of other neurodegenerative diseases, such as Alzheimer's disease or frontotemporal lobar degeneration. The study protocol was approved by the institutional review boards and informed consent was obtained from all participants before evaluation.

2.2 MRI

A 3.0-T MR system (Achieva; Philips Healthcare, Best, The Netherlands) was used for all imaging. Diffusion-weighted images (DWIs) were obtained with a spin-echo echo planar imaging (EPI) sequence consisting of two b values (1,000 and 2,000 s/mm²) acquired along 32 isotropic diffusion gradients in the anterior–posterior phase-encoding direction. Each DWI acquisition was complemented with a gradient-free image (b = 0). Standard and reverse phase-encoded blipped images with no diffusion weighting (Blip Up and Blip Down) were also acquired to correct magnetic susceptibility-induced distortions related to the EPI

acquisitions [12, 13]. The sequence parameters were as follows: repetition time, 9,810 ms; echo time, 100 ms; diffusion gradient pulse duration (δ), 26.4 ms; diffusion gradient separation (Δ), 50.6 ms; field of view, 256×256 mm; matrix size, 128×128 ; slice thickness, 2 mm; and acquisition time, 13 min.

2.3 Diffusion MRI pre-processing

All original DWI datasets were checked visually for each direction from 32 different axial, sagittal, and coronal directions. No dataset had severe artifacts (e.g., gross geometric distortion, signal dropout, or bulk motion). All DWIs were corrected for susceptibility-induced geometric distortions, eddy current distortions, and inter-volume subject motion using the EDDY and TOPUP toolboxes [13]. Next, the resulting DWI data were fitted to the NODDI model [8] using the NODDI Matlab Toolbox5 (http://www.nitrc.org/projects/noddi_toolbox). Vic, OD, and isotropic volume fraction (Viso) maps were generated by Accelerated Microstructure Imaging via Convex Optimization (AMICO) [14]. Only DWIs with $b = 0$ and $1,000 \text{ s/mm}^2$ were used for DTI fitting because DTI indices (FA, mean diffusivity [MD], axial diffusivity [AD], and radial diffusivity [RD]) can be estimated using a conventional monoexponential model [15]. FA, MD, AD, and RD maps for all subjects were calculated using the tool DTIFIT implemented in FMRIB Software Library 5.0.9 (FSL, Oxford Centre for Functional MRI of the Brain, UK;

www.fmrib.ox.ac.uk/fsl) to fit a tensor model to each voxel of the DWI data.

2.4 Tractography

Only the $b = 0$ and $1,000 \text{ s/mm}^2$ datasets of the diffusion-weighted data were used to generate tractography. To achieve successful visualization of the small fibers, DWIs were subjected to up-sampling with trilinear interpolation to 1 mm^3 resolution in MATLAB (version 7.9.0; The Mathworks, Inc., Natick, MA, USA), based on a published protocol [16, 17]. The nigrostriatal tract (as the tract of interest) and the corticospinal tract (CST) (as the control tract) were visualized and analyzed with TrackVis version 0.6.0.1 (<http://www.trackvis.org/>). Earlier, the Diffusion Toolkit version 0.6.3 was used to reconstruct DWIs and generate fiber track data for visualization by TrackVis. The modified fiber assignment by a continuous tracking algorithm was used to obtain optimal visualization of the tract, with an FA threshold of 0.2, angle threshold of 60° for nigrostriatal and of 35° for corticospinal tractography, and default step length of 0.1 mm [16, 18]. Then, to isolate the tracts, regions of interest (ROIs) were applied in the designated areas by two authors (C.A. and M.N.), who were blinded to the disease status of the subjects. Finally, point-to-point profiles of the indices along the segmented tracts were extracted using MATLAB and FSL.

2.4.1 Nigrostriatal tractography

To isolate the nigrostriatal tract, ROIs were placed in the SN and globus pallidus (GP). A nigrofugal tracing study demonstrated that nigrostriatal projections traverse the GP to synapse directly in the striatum. Moreover, striatomesencephalic fibers from the posterior putamen have been found to form a discrete bundle coursing through the GP to converge at the SN [16].

At first, a 3-mm-diameter sphere seed ROI was placed on the ventral SN, which was identified on the anterior midbrain as a green structure on the color FA map from the axial view, inferior to the level of the red nucleus (Fig. 1a). Second, a 4-mm-diameter sphere target ROI was placed in the inferomedial GP, which was identified on the axial and coronal views of the B0 map (Fig. 1b-c). The seed ROI was moved marginally until the streamlines reached the designated target (Fig. 1d) [17].

As previously mentioned, degeneration of dopaminergic neurons is assumed to be a retrograde process. To validate this assumption, the tract was segmented into the upper (from the midpoint to GP) and lower portions (from the midpoint to SNpc). The midpoint of the tract was determined as the point at which the fiber orientation changed as marked by color changes from green (anterior-posterior direction) to red (transverse direction) (Fig. 1e) [17]. However, the entire length of the tract was not analyzed. Similar to previous studies, the length of the tracts were highly variable and the majority terminated beyond ROIs [16, 17]. In

this study, the length of the tracts was set to 10 mm proximal (lower part) and 10 mm distal (upper part) from the midpoint.

2.4.2 Corticospinal tractography

To isolate the CST, the seed and target ROIs were manually drawn on the primary motor cortex and cerebral peduncle, respectively, on the axial view of the B0 map (Supplementary Fig. 1) [18]. Fibers that did not correspond to the CST based on anatomic knowledge were excluded by slight adjustment of ROIs [18]. The whole tract between the seed and target ROIs was then analyzed.

2.5 Statistical analysis

Statistical analyses were performed using IBM SPSS Statistics for Windows, Version 22.0 (IBM Corp., Armonk, NY, USA). The Kolmogorov–Smirnov test was used for analysis of normally distributed data, which included all demographic and clinical variables. The demographic and clinical data were analyzed with the Student's *t*-test for continuous variables and the χ^2 test for categorical variables. The threshold of statistical significance was set at $p < 0.05$.

PD exhibits symptom unilaterality at the onset of disease. The dominant symptoms were strongly correlated with dopaminergic neuron loss in the contralateral hemisphere [19].

Thus, comparisons were made between the contralateral, ipsilateral, and both sides of the nigrostriatal tracts in accordance with the patient's dominant side, while for the control tract, comparisons were made between both sides of the tracts of PD patients and healthy controls.

The unpaired *t*-test was used to assess differences in ROIs of the FA, MD, AD, RD, Vic, OD, and Viso maps between groups. The Bonferroni correction was used for multiple comparisons ($n = 63$: [proximal, distal, and whole] \times [FA, MD, AD, RD, Vic, OD, and Viso] \times [contralateral, ipsilateral, and bilateral], with a level of significance of $p < 0.05/63 = 0.000794$). To evaluate the strength of the relationship between the group comparisons, the effect size was calculated according to Cohen's definition (Cohen's *d*). The Pearson correlation test was used to identify correlations between each diffusion parameter and disease duration or severity, as measured by the motor score of Unified Parkinson's Disease Rating Scale (UPDRS)-III. A two-tailed *p*-value of < 0.05 was considered to indicate significance.

To validate the reproducibility of the data, nigrostriatal and corticospinal tractography were performed twice by different examiners. In addition, DTI and NODDI indices from the first and second tractography were compared with the intra-class correlation coefficient (ICC).

3. Results

There were no significant differences in the distribution of age ($p = 0.483$, Student's t -test) and sex ($p = 1.000$, χ^2 test) between PD patients and healthy controls (Table 1).

The contralateral distal Vic ($p = 0.00028$; Cohen's d : 1.05; effect-size: 0.46) was significantly lower in PD patients than in healthy controls (Fig. 2, Supplementary Table 1).

There were no indices that were significantly altered in the proximal part (Fig. 2, Supplementary Table 1). The tract profile of the contralateral Vic of the NSP also demonstrated significantly altered distal portion, as compared with the proximal portion (Fig. 3). In comparison, no indices were significantly altered in the CST of PD patients compared with the healthy controls (Supplementary Table 2). Further, no correlations were detected between any of the indices and disease duration or motor symptom severity, as assessed with UPDRS-III.

In general, nigrostriatal and corticospinal tractography, and measurements of DTI and NODDI indices had good reproducibility. The ICCs of nigrostriatal tractography were distal FA, 0.898; proximal FA, 0.809; distal Vic, 0.828; proximal Vic, 0.821; distal OD, 0.889; proximal OD, 0.707; distal ISO, 0.825; proximal ISO, 0.870; distal AD, 0.927; proximal AD, 0.934; distal RD, 0.853; proximal RD, 0.888; distal MD, 0.876; and proximal MD, 0.894. The ICCs of corticospinal tractography were FA, 0.851; Vic, 0.910; OD, 0.882; ISO, 0.939; AD, 0.981; RD, 0.994; and MD, 0.995.

4. Discussion

The contralateral distal Vic of the NSP was significantly decreased in PD patients compared with healthy controls. The reduced Vic values of the NSP in PD patients indicated a neurite density reduction, which is consistent with histopathological studies suggesting that up to 70% of dopamine neurons have been lost by the time of the first diagnosis [2]. The accumulation of α -Synuclein protein in the form of Lewy bodies and neurites may also impair axonal transport, which leads to neuronal loss, and have also been shown to impair neurite outgrowth and branching [3-6]. A significant decrease in the contralateral Vic is consistent with the well-established fact that asymmetrical motor symptoms are exhibited at the time of diagnosis with greater dopaminergic neuron depletion on the contralateral side [19]. Meanwhile, a significant decrease in Vic on the distal part of the NSP supports the “dying back” process of PD [2, 4, 20]. Studies of animal models of PD indicate that axon terminal loss occurs several weeks before the loss of SN dopaminergic neurons [20]. It was estimated that approximately 50%–70% of striatal dopaminergic terminals and 30% of SN dopaminergic neurons are lost by the time symptoms appear [4, 20]. This finding might be useful to identify alterations during the early course of the disease when changes have not been detected in the proximal portion of the tract or SN.

Although not statistically significant, there was a trend suggesting that the contralateral distal Viso, MD, RD, and AD were higher in PD patients than in healthy

controls with greater differences compared with the proximal part (Fig. 2, Supplementary Table 2). Increased Viso, MD, RD, and AD values in PD indicate axonal degeneration in PD, which is characterized by the accumulation of water content and increased spacing between membrane layers due to neuronal loss, which promoted accelerated water movement [9]. These findings support that neuronal loss was more prominent on the distal part of the NSP and also the “dying back” process.

FA values of the NSP of PD patients in this study were not significantly decreased. These findings are in contrast to those of previous studies from Tan et al. [16] and Zhang et al. [17], which showed significantly reduced FA values of the NSP of PD patients. Conflicting findings between the present study and previous studies may be related to discrepancies in symptom severity across the studies. PD patient groups in the studies by Tan et al. [16] and Zhang et al. [17] displayed higher motor symptom severity (UPDRS-III motor scores), as compared with the present study. Therefore, it is possible that more severe degeneration of the NSP underlies greater motor symptom severity. In contrast, another study of the NSP by Hikishima et al. [21] showed non-significant increased FA in a marmoset model of PD that was treated with 1-methyl-4-phenyl-1,2,3,6-tetrahydropyridine (MPTP). However, a study of patients with MPTP-induced parkinsonism showed different pathological findings. Lewy pathology, which is the histopathological hallmark of PD, was not found in MPTP-induced parkinsonism [22], suggesting that the assumption of NSP degeneration in MPTP-induced

parkinsonism may be different from idiopathic PD [22]. Therefore, it is difficult to simply compare these results with those of other studies of idiopathic PD.

Previously, Kamagata et al. [9] performed an ROI study on the SN and basal ganglia of 58 PD patients, which showed a significant decrease in Vic in the contralateral SNpc and putamen. Compared with the ROI approach, in which structures of interest are manually defined and analyzed, tractography enabled us to clearly identify the NSP and measure diffusion indices more precisely with higher reproducibility [23]. Therefore, we assumed that direct measurement of the NSP might be more valuable for the clinical assessment of PD because degeneration of the NSP is the major cause of motor symptoms. Moreover, dopamine neurons in the SNpc are not only projected to the stratum but some are also projected to the prefrontal cortex [24] and even though the striatum was mostly composed of medium spiny neurons that act as dopamine receptors, the remaining spiny neurons also contain cholinergic and somatostatin neurons [25]. Furthermore, iron accumulation in the SN and striatum of PD patients may influence DTI indices, including a reduction of MD and an elevation of FA [26, 27]. Also, accurate quantification of neurite density, as represented by Vic, in the iron-rich structure is difficult to achieve because of the low signal-to-noise ratio [28]. Therefore, the examination of the NSP will show the actual microstructural changes to the dopaminergic neurons caused by PD without any interference from iron deposition, and by examining the NSP, a retrograde degeneration can be evaluated.

None of the indices in this study were correlated with disease duration. This finding is consistent with histopathological studies showing that axonal degeneration in PD occurs before the appearance of symptoms [2, 20]. Meanwhile, the fact that none of the indices correlated with the UPDRS-III indicates that diffusion alterations do not align with the worsening of motor function, possibly due to the effect of the medication [29]. This observation is in line with the findings of Zhang et al. [8] and Wen et al. [30], which reported correlations between DTI indices and UPDRS-III in the brain of untreated PD patients and a study by Lenfeldt et al. [29], which showed no correlation in the SN and basal ganglia of treated PD patients. In contrast, Kamagata et al. [12] revealed significant negative correlations between Vic and ODI in the SNpc and putamen with disease severity in a group of treated PD patients. However, the type and dosage of the medication and the severity of motor symptoms have might lead to the discrepancy

In the present study, we also isolated and analyzed CST as a control tract. Previous histopathological [31] and imaging [32] studies have demonstrated that CST is relatively unaffected in PD. In line with those studies, our study also showed that DTI and NODDI indices in the CST were not significantly altered in PD patients compared with healthy controls, confirming the validity of our methodology and showing that the pathology of PD is mainly confined in the NSP.

This study has the following limitations: 1) ROIs of the tractography in the NSP

determination were created manually, thus basic knowledge of brain anatomy was required to place ROIs in the appropriate locations; otherwise, the NSP was difficult to visualize.

Moreover, the adjacent fiber tracts around the NSP also complicated identification of the correct tract [17]. However, repeated measurements performed by different raters exhibited good reproducibility with an ICC of 0.707–0.934; 2) diffusion-based tractography is unable to differentiate the directionality of the tracts and the isolated tracts may include anterograde nigrostriatal-nigropallidal and retrograde palidonigral thalamonigral pathways [16]; and 3) this study was conducted on a small sample size; thus, further prospective and longitudinal studies with larger sample sizes are required to validate the correlation between NODDI indices, disease duration, and clinical severity.

5. Conclusion

NODDI analysis of the NSP provided results that likely reflect a decreased neurite density in the distal NSP of PD patients. This finding is consistent with histopathological studies suggesting that the degeneration of dopamine neurons in PD is a “dying back” process, beginning from the presynaptic terminals and the distal axons. Therefore, NODDI might provide complementary information to the DTI and should be jointly used to reveal the microstructural changes in the NSP of PD.

Author contributions

C. Andica designed the study, analyzed the data, and wrote and revised the manuscript. K.

Kamagata and T. Hatano designed the study, analyzed the data, and revised the manuscript. A.

Saito, M. Nakazawa, and R. Ueda contributed to data acquisition and interpretation, and

revised the manuscript. A. Okuzumi, Y. Motoi, K. Kamiya, M. Suzuki, M. Hori, K. K.

Kumamaru, N. Hattori, and S. Aoki analyzed the data and revised the manuscript. Statistical

analysis was conducted by C. Andica and K. Kamagata. All authors have read and approved

the final version of the manuscript.

Study funding

This study was supported by Hitachi, Ltd., by the program for Brain Mapping by Integrated

Neurotechnologies for Disease Studies (Brain/MINDS) from the Japan Agency for Medical

Research and Development (AMED) and by the Japan Society for the Promotion of Science

(JSPS) KAKENHI (grant number JP16K19854).

Conflict of interest

The authors have no conflicts of interest to declare.

Acknowledgments

We are grateful to Dr. Shuko Nojiri for assistance with the statistical analysis.

References

- [1] Burke RE, O'Malley K. Axon degeneration in Parkinson's disease. *Exp Neurol*. 2013;246:72-83. doi:10.1016/j.expneurol.2012.01.011.
- [2] Cheng HC, Ulane CM, Burke RE. Clinical progression in Parkinson disease and the neurobiology of axons. *Ann Neurol*. 2010;67(6):715-25. doi:10.1002/ana.21995.
- [3] Braak H, Sandmann-Keil D, Gai W, Braak E. Extensive axonal Lewy neurites in Parkinson's disease: a novel pathological feature revealed by alpha-synuclein immunocytochemistry. *Neurosci Lett*. 1999;265(1):67-9.
- [4] Koch JC, Bitow F, Haack J, d'Hedouville Z, Zhang JN, Tonges L et al. Alpha-Synuclein affects neurite morphology, autophagy, vesicle transport and axonal degeneration in CNS neurons. *Cell Death Dis*. 2015;6:e1811. doi:10.1038/cddis.2015.169.
- [5] Volpicelli-Daley LA, Gamble KL, Schultheiss CE, Riddle DM, West AB, Lee VM. Formation of alpha-synuclein Lewy neurite-like aggregates in axons impedes the transport of distinct endosomes. *Mol Biol Cell*. 2014;25(25):4010-23. doi:10.1091/mbc.E14-02-0741.
- [6] Perlson E, Maday S, Fu MM, Moughamian AJ, Holzbaur EL. Retrograde axonal transport: pathways to cell death? *Trends Neurosci*. 2010;33(7):335-44. doi:10.1016/j.tins.2010.03.006.
- [7] Kamagata K, Hatano T, Aoki S. What is NODDI and what is its role in Parkinson's assessment? *Expert Rev Neurother*. 2016;16(3):241-3. doi:10.1586/14737175.2016.1142876.

- [8] Zhang H, Schneider T, Wheeler-Kingshott CA, Alexander DC. NODDI: practical in vivo neurite orientation dispersion and density imaging of the human brain. *Neuroimage*. 2012;61(4):1000-16. doi:10.1016/j.neuroimage.2012.03.072.
- [9] Kamagata K, Hatano T, Okuzumi A, Motoi Y, Abe O, Shimoji K et al. Neurite orientation dispersion and density imaging in the substantia nigra in idiopathic Parkinson disease. *Eur Radiol*. 2016;26(8):2567-77. doi:10.1007/s00330-015-4066-8.
- [10] Hughes AJ, Daniel SE, Kilford L, Lees AJ. Accuracy of clinical diagnosis of idiopathic Parkinson's disease: a clinico-pathological study of 100 cases. *J Neurol Neurosurg Psychiatry*. 1992;55(3):181-4.
- [11] Hoehn MM, Yahr MD. Parkinsonism: onset, progression and mortality. *Neurology*. 1967;17(5):427-42.
- [12] Andersson JL, Skare S, Ashburner J. How to correct susceptibility distortions in spin-echo echo-planar images: application to diffusion tensor imaging. *NeuroImage*. 2003;20(2):870-88. doi:10.1016/S1053-8119(03)00336-7.
- [13] Andersson JL, Sotiropoulos SN. An integrated approach to correction for off-resonance effects and subject movement in diffusion MR imaging. *Neuroimage*. 2016;125:1063-78. doi:10.1016/j.neuroimage.2015.10.019.
- [14] Daducci A, Canales-Rodriguez EJ, Zhang H, Dyrby TB, Alexander DC, Thiran JP. Accelerated Microstructure Imaging via Convex Optimization (AMICO) from diffusion MRI

data. *Neuroimage*. 2015;105:32-44. doi:10.1016/j.neuroimage.2014.10.026.

[15] Basser PJ, Mattiello J, LeBihan D. Estimation of the effective self-diffusion tensor from the NMR spin echo. *J Magn Reson B*. 1994;103(3):247-54.

[16] Tan WQ, Yeoh CS, Rumpel H, Nadkarni N, Lye WK, Tan EK et al. Deterministic Tractography of the Nigrostriatal-Nigropallidal Pathway in Parkinson's Disease. *Sci Rep*. 2015;5:17283. doi:10.1038/srep17283.

[17] Zhang Y, Wu IW, Buckley S, Coffey CS, Foster E, Mendick S et al. Diffusion tensor imaging of the nigrostriatal fibers in Parkinson's disease. *Mov Disord*. 2015;30(9):1229-36. doi:10.1002/mds.26251.

[18] Bigourdan A, Munsch F, Coupe P, Guttmann CR, Sagnier S, Renou P et al. Early Fiber Number Ratio Is a Surrogate of Corticospinal Tract Integrity and Predicts Motor Recovery After Stroke. *Stroke*. 2016;47(4):1053-9. doi:10.1161/STROKEAHA.115.011576.

[19] Blesa J, Juri C, Garcia-Cabezas MA, Adanez R, Sanchez-Gonzalez MA, Cavada C et al. Inter-hemispheric asymmetry of nigrostriatal dopaminergic lesion: a possible compensatory mechanism in Parkinson's disease. *Front Syst Neurosci*. 2011;5:92. doi:10.3389/fnsys.2011.00092.

[20] Tagliaferro P, Burke RE. Retrograde Axonal Degeneration in Parkinson Disease. *J Parkinsons Dis*. 2016;6(1):1-15. doi:10.3233/JPD-150769.

[21] Hikishima K, Ando K, Yano R, Kawai K, Komaki Y, Inoue T et al. Parkinson Disease:

Diffusion MR Imaging to Detect Nigrostriatal Pathway Loss in a Marmoset Model Treated with 1-Methyl-4-phenyl-1,2,3,6-tetrahydropyridine. *Radiology*. 2015;275(2):430-7.

doi:10.1148/radiol.14140601.

[22] Langston JW, Forno LS, Tetrud J, Reeves AG, Kaplan JA, Karluk D. Evidence of active nerve cell degeneration in the substantia nigra of humans years after

1-methyl-4-phenyl-1,2,3,6-tetrahydropyridine exposure. *Ann Neurol*. 1999;46(4):598-605.

[23] Taoka T, Kin T, Nakagawa H, Hirano M, Sakamoto M, Wada T et al. Diffusivity and diffusion anisotropy of cerebellar peduncles in cases of spinocerebellar degenerative disease.

Neuroimage. 2007;37(2):387-93. doi:10.1016/j.neuroimage.2007.05.028.

[24] Puig MV, Rose J, Schmidt R, Freund N. Dopamine modulation of learning and memory in the prefrontal cortex: insights from studies in primates, rodents, and birds. *Front Neural*

Circuits. 2014;8:93. doi:10.3389/fncir.2014.00093.

[25] Standring S. *Gray's anatomy: the anatomical basis of clinical practice*. Fortieth edition ed. New York: Elsevier limited; 2008.

[26] Wang JY, Zhuang QQ, Zhu LB, Zhu H, Li T, Li R et al. Meta-analysis of brain iron

levels of Parkinson's disease patients determined by postmortem and MRI measurements. *Sci*

Rep. 2016;6:36669. doi:10.1038/srep36669.

[27] Xu X, Wang Q, Zhong J, Zhang M. Iron deposition influences the measurement of water diffusion tensor in the human brain: a combined analysis of diffusion and iron-induced phase

changes. *Neuroradiology*. 2015;57(11):1169-78. doi:10.1007/s00234-015-1579-4.

[28] Surova Y, Lampinen B, Nilsson M, Latt J, Hall S, Widner H et al. Alterations of Diffusion Kurtosis and Neurite Density Measures in Deep Grey Matter and White Matter in Parkinson's Disease. *PLoS One*. 2016;11(6):e0157755. doi:10.1371/journal.pone.0157755.

[29] Lenfeldt N, Hansson W, Larsson A, Nyberg L, Birgander R, Forsgren L. Diffusion tensor imaging and correlations to Parkinson rating scales. *J Neurol*. 2013;260(11):2823-30. doi:10.1007/s00415-013-7080-2.

[30] Wen MC, Heng HS, Ng SY, Tan LC, Chan LL, Tan EK. White matter microstructural characteristics in newly diagnosed Parkinson's disease: An unbiased whole-brain study. *Sci Rep*. 2016;6:35601. doi:10.1038/srep35601.

[31] Braak H, Del Tredici K, Rub U, de Vos RA, Jansen Steur EN, Braak E. Staging of brain pathology related to sporadic Parkinson's disease. *Neurobiol Aging*. 2003;24(2):197-211.

[32] Hattori T, Orimo S, Aoki S, Ito K, Abe O, Amano A et al. Cognitive status correlates with white matter alteration in Parkinson's disease. *Hum Brain Mapp*. 2012;33(3):727-39. doi:10.1002/hbm.21245.

Figure captions:

Figure 1. Steps for isolating the nigrostriatal pathway. In the midbrain, a 3–mm-diameter sphere seed ROI was placed in the ventral of substantia nigra (SN) which appears green on the (A) axial color FA map. In the basal ganglia, a 4–mm-diameter sphere target ROI was placed in the inferomedial globus pallidus (GP) that was identified on the (B) axial and (C) coronal view of the B0 map. To isolate the tract (D), the seed ROI was moved until the streamlines reached the designated target. For analysis, the midpoint of the tract (yellow line) was determined by fiber orientation changes as marked by color changes from green (anterior–posterior) to red (transverse). The midpoint (yellow line) to the GP was determined as the upper part and the midpoint (yellow line) to the SN as the lower part.

Figure 2. Mean values of intracellular volume fraction (V_{ic}), orientation dispersion index (OD), isotropic volume fraction (V_{iso}), fractional anisotropy (FA), mean diffusivity (MD), radial diffusivity (RD), and axial diffusivity (AD) of the nigrostriatal pathway in Parkinson's disease (PD) patients (gray bars) and healthy controls (white bars). *Contralateral distal V_{ic} values significantly differed ($p < 0.000794$) between PD patients and healthy controls.

Figure 3. Tract profiles of the intracellular volume fraction (V_{ic}) of the contralateral nigrostriatal pathway (NSP) for Parkinson's disease (PD) patients and healthy controls (HC).

The distal (gray area) and proximal portions (white area) of the NSP were evaluated. The Vic values of the distal regions of the NSP were significantly lower in PD patients than in the HCs.

Table 1. Demographic characteristics of the subjects

	Healthy controls	PD patients	<i>P</i> value
Number	29	29	
Sex (male/female)	14/15	14/15	1.000
Age (years)	65.52 ± 11.87	67.79 ± 10.00	0.483
Disease duration (years)	NA	6.24 ± 3.40	
UPDRS-III Motor Score	NA	15.93 ± 9.18	
Hoehn-Yahr stage	NA	1.97 ± 0.68	

PD, Parkinson disease; *NA*, not applicable; *UPDRS-III*, Unified Parkinson's Disease Rating Scale-III

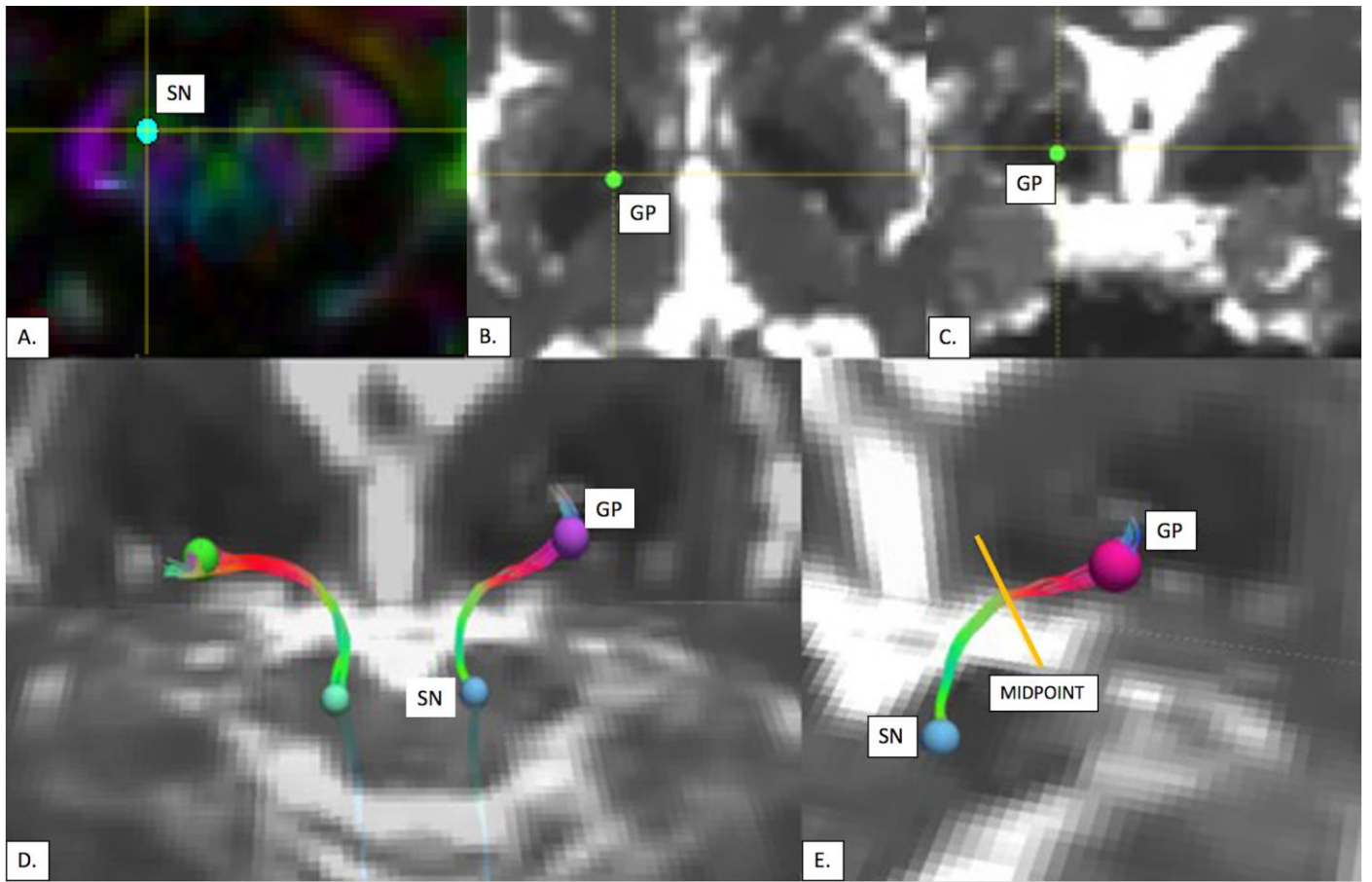


Figure 1

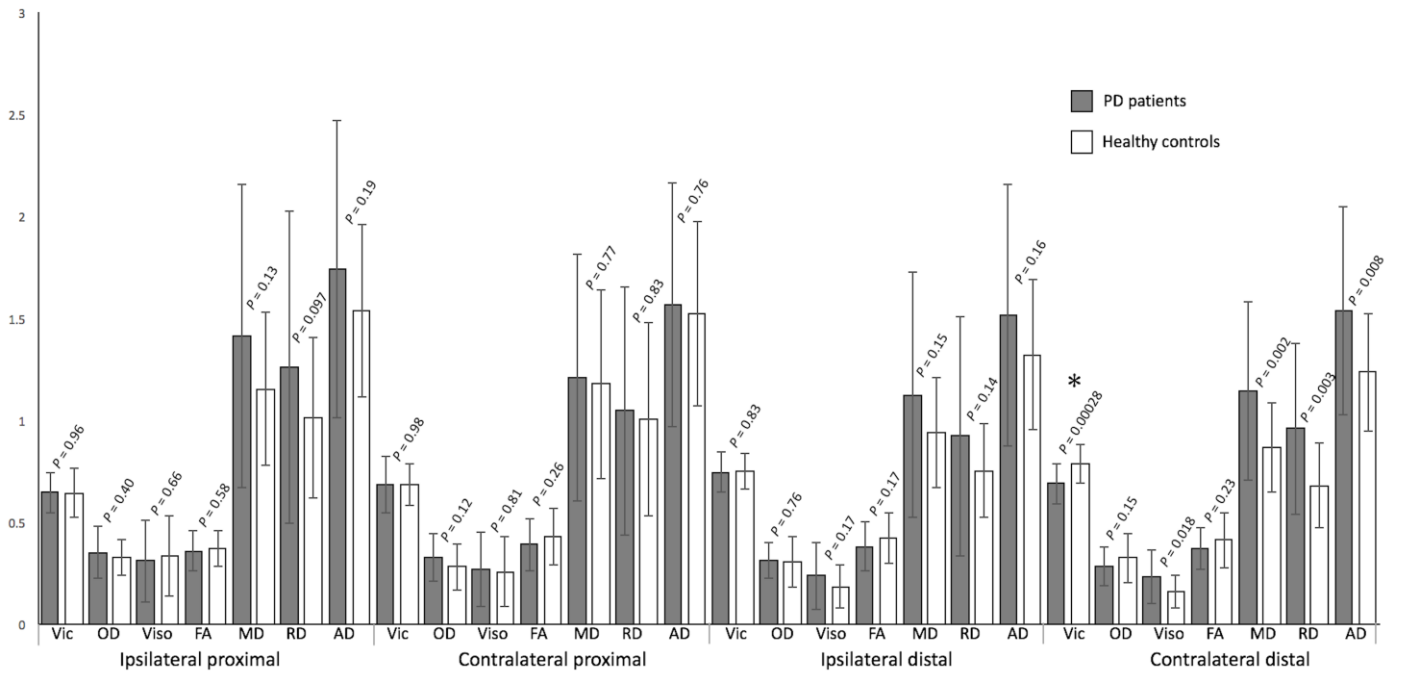


Figure 2

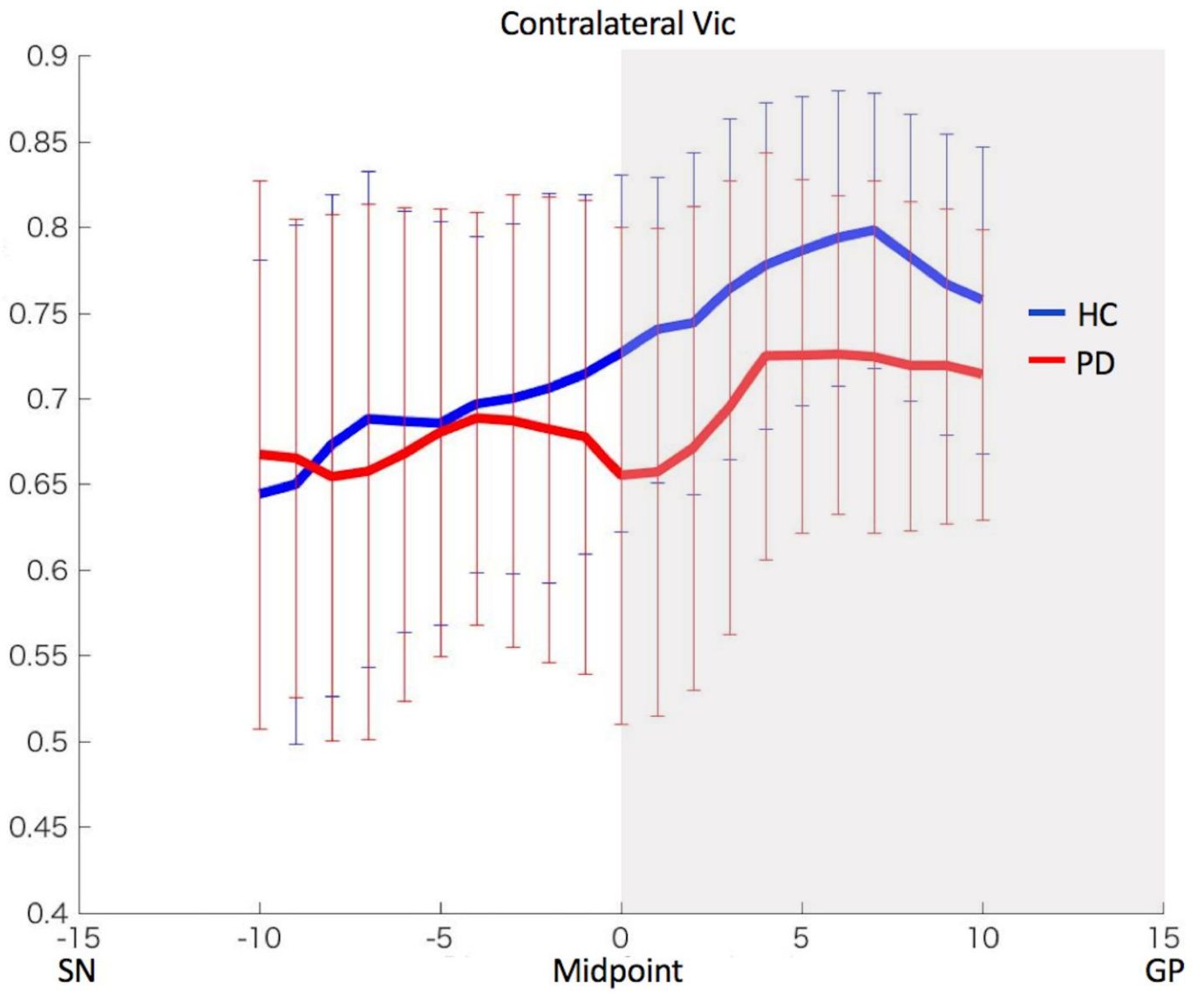


Figure 3

Supplementary Table 1. Diffusion parameters of the nigrostriatal pathway (NSP) of PD patients and healthy controls

	Healthy controls (<i>n</i> = 29)	PD patients (<i>n</i> = 29)	<i>P</i> -value	Cohen's <i>d</i>	Effect-size <i>r</i>
Vic					
Ipsilateral whole		0.69 (±0.085)	0.70	0	0
Contralateral whole		0.68 (±0.11)	0.24	0.29	0.15
Bilateral whole	0.70 (±0.067)	0.68 (±0.075)	0.29	0.28	0.14
Ipsilateral distal		0.75 (±0.097)	0.83	0	0
Contralateral distal		0.69 (±0.098)	0.00028*	1.05	0.46
Bilateral distal	0.77 (±0.076)	0.72 (±0.063)	0.007	0.72	0.34
Ipsilateral proximal		0.64 (±0.096)	0.96	0	0
Contralateral proximal		0.68 (±0.14)	0.98	0	0
Bilateral proximal	0.66 (±0.082)	0.66 (±0.089)	0.99	0	0
OD					
Ipsilateral whole		0.33 (±0.091)	0.61	-0.24	-0.12
Contralateral whole		0.32 (±0.097)	0.15	-0.41	-0.20
Bilateral whole	0.30 (±0.066)	0.32 (±0.063)	0.16	-0.31	-0.15
Ipsilateral distal		0.31 (±0.086)	0.76	-0.095	-0.047
Contralateral distal		0.28 (±0.092)	0.15	0.37	0.18
Bilateral distal	0.31 (±0.11)	0.30 (±0.070)	0.51	0.11	0.054
Ipsilateral proximal		0.35 (±0.13)	0.40	-0.18	-0.090
Contralateral proximal		0.33 (±0.12)	0.12	-0.42	-0.20
Bilateral proximal	0.30 (±0.077)	0.34 (±0.086)	0.094	-0.49	-0.24

Viso

Ipsilateral whole		0.29 (± 0.16)	0.73	-0.066	-0.033
Contralateral whole		0.26 (± 0.14)	0.28	-0.24	-0.12
Bilateral whole	0.25 (± 0.11)	0.28 (± 0.12)	0.40	-0.26	-0.13
Ipsilateral distal		0.24 (± 0.17)	0.17	-0.42	-0.21
Contralateral distal		0.23 (± 0.13)	0.018	-0.64	-0.31
Bilateral distal	0.17 (± 0.084)	0.23 (± 0.13)	0.034	-0.55	-0.26
Ipsilateral proximal		0.31 (± 0.20)	0.66	0.10	0.050
Contralateral proximal		0.27 (± 0.18)	0.81	-0.057	-0.028
Bilateral proximal	0.29 (± 0.15)	0.29 (± 0.14)	0.87	0	0

FA

Ipsilateral whole		0.37 (± 0.097)	0.18	0.34	0.17
Contralateral whole		0.38 (± 0.098)	0.046	0.55	0.26
Bilateral whole	0.42 (± 0.085)	0.37 (± 0.082)	0.045	0.60	0.29
Ipsilateral distal		0.38 (± 0.12)	0.17	0.33	0.16
Contralateral distal		0.37 (± 0.10)	0.23	0.34	0.17
Bilateral distal	0.42 (± 0.12)	0.37 (± 0.099)	0.16	0.45	0.22
Ipsilateral proximal		0.36 (± 0.099)	0.58	0.11	0.05
Contralateral proximal		0.39 (± 0.13)	0.26	0.30	0.15
Bilateral proximal	0.40 (± 0.090)	0.37 (± 0.085)	0.25	0.34	0.17

MD

Ipsilateral whole		1.31 (± 0.63)	0.11	-0.44	-0.21
Contralateral whole		1.18 (± 0.50)	0.31	-0.28	-0.14

Bilateral whole	1.07 (± 0.30)	1.24 (± 0.44)	0.10	-0.45	-0.22
Ipsilateral distal		1.12 (± 0.60)	0.15	-0.39	-0.19
Contralateral distal		1.14 (± 0.44)	0.002	-0.80	-0.37
Bilateral distal	0.90 (± 0.21)	1.13 (± 0.44)	0.12	-0.67	-0.32
Ipsilateral proximal		1.41 (± 0.75)	0.13	-0.44	-0.21
Contralateral proximal		1.21 (± 0.60)	0.77	-0.056	-0.028
Bilateral proximal	1.16 (± 0.38)	1.31 (± 0.49)	0.22	-0.34	v0.17
RD					
Ipsilateral whole		1.13 (± 0.63)	0.093	-0.44	-0.22
Contralateral whole		0.99 (± 0.50)	0.33	-0.25	-0.13
Bilateral whole	0.90 (± 0.30)	1.06 (± 0.43)	0.088	-0.43	-0.21
Ipsilateral distal		0.92 (± 0.59)	0.14	-0.38	-0.19
Contralateral distal		0.96 (± 0.42)	0.003	-0.84	-0.39
Bilateral distal	0.71 (± 0.19)	0.94 (± 0.43)	0.014	-0.69	-0.33
Ipsilateral proximal		1.26 (± 0.76)	0.097	-0.40	-0.19
Contralateral proximal		1.05 (± 0.61)	0.83	-0.091	-0.045
Bilateral proximal	1.01 (± 0.38)	1.15 (± 0.50)	0.21	-0.32	-0.16
AD					
Ipsilateral whole		1.62 (± 0.69)	0.25	-0.29	-0.14
Contralateral whole		1.52 (± 0.56)	0.40	-0.21	-0.10
Bilateral whole	1.44 (± 0.33)	1.57 (± 0.54)	0.25	-0.29	-0.14
Ipsilateral distal		1.52 (± 0.64)	0.16	-0.38	-0.19
Contralateral distal		1.53 (± 0.51)	0.008	-0.70	-0.33

Bilateral distal	1.28 (± 0.29)	1.53 (± 0.49)	0.023	-0.62	-0.30
Ipsilateral proximal		1.74 (± 0.73)	0.19	-0.35	-0.17
Contralateral proximal		1.57 (± 0.60)	0.76	-0.094	-0.047
Bilateral proximal	1.53 (± 0.38)	1.65 (± 0.52)	0.30	-0.26	-0.13

Vic, intracellular volume fraction (dimensionless); *OD*, orientation dispersion index (dimensionless); *Viso*, isotropic volume fraction (dimensionless); *FA*, fractional anisotropy (dimensionless); *MD*, mean diffusivity (mm^2/s); *RD* radial diffusivity (mm^2/s); *AD*, axial diffusivity (mm^2/s). * Statistical difference between PD patients and healthy controls ($P < 0.000794$).

Supplementary Table 2. Diffusion parameters of the corticospinal tract (CST) of PD patients and healthy controls

	Healthy controls ($n = 29$)	PD patients ($n = 29$)	<i>P</i> -value	Cohen's d	Effect-size <i>r</i>
<i>Vic</i>	0.72 (± 0.021)	0.70 (± 0.032)	0.04	0.74	0.35
<i>OD</i>	0.14 (± 0.020)	0.14 (± 0.022)	0.14	0	0
<i>Viso</i>	0.12 (± 0.014)	0.11 (± 0.017)	0.15	0.64	0.31
<i>FA</i>	0.59 (± 0.037)	0.58 (± 0.035)	0.067	0.28	0.14
<i>MD</i>	0.40 (± 0.037)	0.42 (± 0.041)	0.86	-0.51	-0.25
<i>RD</i>	0.67 (± 0.056)	0.68 (± 0.072)	0.85	-0.16	-0.077
<i>AD</i>	1.22 (± 0.13)	1.18 (± 0.15)	0.35	0.28	0.14

Vic, intracellular volume fraction (dimensionless); *OD*, orientation dispersion index (dimensionless); *Viso*, isotropic volume fraction (dimensionless); *FA*, fractional anisotropy (dimensionless); *MD*, mean diffusivity (mm^2/s); *RD* radial diffusivity (mm^2/s); *AD*, axial

diffusivity (mm^2/s).

Supplementary Figure Captions

Supplementary Figure 1. Steps for isolating the corticospinal tract. On the axial view of the B0 map, first, a seed ROI was manually drawn on the primary motor cortex (A). Then, a target ROI was drawn on the cerebral peduncle (B). Fibers that did not correspond to the corticospinal tract based on anatomic knowledge were excluded by slight adjustment of the ROIs.

